Generation of Dicke States with Phonon-Mediated Multilevel Stimulated Raman Adiabatic Passage

Atsushi Noguchi,* Kenji Toyoda, and Shinji Urabe

Graduate School of Engineering Science, Osaka University, 1-3 Machikaneyama, Toyonaka, Osaka 5608531, Japan
(Received 5 September 2012; published 27 December 2012)

We generate half-excited symmetric Dicke states of two and four ions. We use multilevel stimulated Raman adiabatic passage whose intermediate states are phonon Fock states. This process corresponds to the spin squeezing operation and half-excited Dicke states are generated during multilevel stimulated Raman adiabatic passage. This method does not require local access for each ion or the preparation of phonon Fock states. Furthermore, it is robust since it is an adiabatic process. We evaluate the Dicke state using a witness operator and determine the upper and lower bounds of the fidelity without using full quantum tomography.

Genuine multipartite entanglement has been extensively investigated in quantum information science [1]. It is very difficult to generate genuine multipartite entanglement because the entangled states of many qubits decay with the square of the qubit number [1]. To date, the Greenberger–Horne–Zeilinger state of 14 qubits has been generated [1] using a Mølmer-Sørensen gate [2]; however, the half-excited symmetric Dicke states that form another important group of entangled states have been generated by photonic qubits with only four and six photons [3,4]. No robust and efficient method has been demonstrated for generating Dicke states using more than two trapped ions [5,6].

Dicke states are generally the simultaneous eigenstates of the total angular momentum operator and its projection along one direction. One subgroup of Dicke states is symmetric under permutation of qubits:

$$|D_n^m\rangle = \frac{1}{\sqrt{_nC_m}}\sum_k \hat{P}_k|\uparrow\uparrow\ldots\uparrow\downarrow\downarrow\ldots\downarrow\rangle,$$

where P_k is the permutation operator and $_nC_m = n!/[m!(n-m)!]$. These states have symmetrically m up spin states of n qubits. In this Letter, we refer to these states as symmetric Dicke states. Here, we focus on an even number of qubits and the half-excited symmetric Dicke states ($|D_{2k}^k\rangle$ with k a positive integer), which are difficult to generate by addressing local qubits with an array of laser pulses [7] or postselection by photodetection with an atomic ensemble [8]. These multipartite entangled states are not only important for quantum information science, they are also useful for precise measurements such as Heisenberg-limited measurements [9–12] because these states are related to the squeezed vacuum state in quantum optics through the two-excitation correlation [13]. Moreover, half-excited symmetric Dicke states can form decoherence-free entangled states with a dressing field [14].

In this Letter, we use phonon-mediated multilevel stimulated Raman adiabatic passage (STIRAP) [15,16] to generate half-excited symmetric Dicke states of two and four ions. We evaluate the four-ion Dicke state with a witness operator and the fidelity without using full quantum tomography.

We consider the case where N ions are cooled to the ground state and are irradiated by two-color laser beams that are detuned from the blue and red sideband transitions for the Mølmer-Sørensen interaction [2]. In the interaction picture, the Hamiltonian is expressed by

$$\hat{H} = \frac{\eta\Omega_r}{2}(\hat{a}\hat{J}_+ e^{-i\delta t} + \hat{a}^\dagger\hat{J}_- e^{i\delta t})$$
$$+ \frac{\eta\Omega_b}{2}(\hat{a}^\dagger\hat{J}_+ e^{i\delta t} + \hat{a}\hat{J}_- e^{-i\delta t}),$$

where $\hat{J}_\pm$ ($= \sum_i \hat{\sigma}_\pm^{(i)}$, where $\hat{\sigma}_\pm^{(i)}$ is the Pauli operator for the ith ion) is the global spin flip operator and $\hat{a}(\hat{a}^\dagger)$ is the annihilation (creation) operator for the center of motion of the ion chain, and δ, $\eta\Omega_{r,b}$ are the detuning and Rabi frequencies of the blue and red sideband transitions. We begin with the initial state $|\downarrow\downarrow\ldots\downarrow\rangle_s |0\rangle_p$, where $|0\rangle_p$ is the phonon vacuum state. This initial state is obviously the dark state of this Hamiltonian when $\Omega_b = 0$ and we adiabatically change the amplitudes of the two-color beams to transfer the population to the other dark states ($|\uparrow\uparrow\ldots\uparrow\rangle_s|0\rangle_p$, where $\Omega_r = 0$). Here, we calculate the dark states and show that the half-excited symmetric Dicke states are the dark states of the Hamiltonian.

We represent the Hamiltonian by the eigenstates of the global spin operators $\hat{J}^2$ and $\hat{J}_z$. Due to the symmetry of the Hamiltonian, we can consider the symmetric subspace of the whole N qubit Hilbert space, whose basis is $|D_N^m\rangle_s|n\rangle_p$, where N is the number of ions and $|n\rangle_p$ denote the phonon Fock states. Figure 1(a) shows the interaction for the lower phonon states ($|0\rangle_p$, $|1\rangle_p$ and $|2\rangle_p$). We assume that the red and blue sideband transitions have the same magnitudes for one-photon detuning δ and that the "vertical" Raman transitions [see Fig. 1(a)] are on resonance relative to
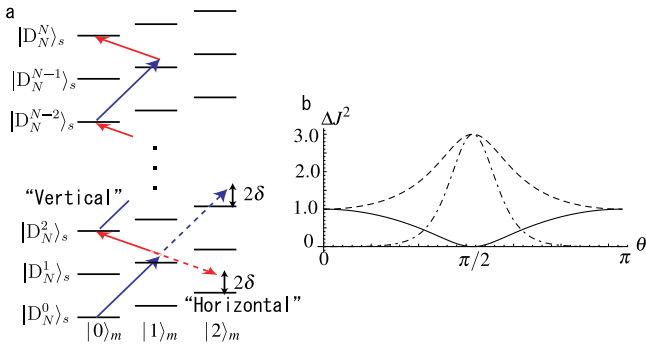
FIG. 1 (color online). (a) Energy-level diagram of phonon-mediated multilevel STIRAP. Vertical ladders indicate spin states and horizontal arrays represent phonon Fock states. (b) Evolution of spin noise for four ions. Solid, dashed, and dot-dashed curves indicate ΔJ_x^2, ΔJ_y^2, and ΔJ_z^2, respectively.

two-photon detuning. On the other hand, there are other Raman transitions, which are "horizontal" Raman transitions [see Fig. 1(a)]; these transitions change the mean phonon number. For the case in which vertical Raman transitions are on resonance, horizontal Raman transitions have two-photon detuning as 2δ. When $2\delta \gg \eta\Omega_r, \eta\Omega_b$, the horizontal Raman transitions can be ignored and the interaction can be expressed in Fig. 1(a) corresponding to the multilevel Raman transitions [6]. The Raman couplings are not independent and they have different strengths due to the cooperative effects of symmetric Dicke states. The coupling strengths of the cooperative effects are expressed by

$$R_m \equiv {}_s\langle D_N^{m+1}|\hat{J}_+|D_N^m\rangle_s = (N-m)\sqrt{\frac{{}_N C_m}{{}_N C_{m+1}}},$$

and the Hamiltonian is expressed as follows in a rotating frame with respect to the COM mode:

$$H = \begin{pmatrix} 0 & R_0\eta\Omega_b & 0 & \cdots & & 0 \\ R_0\eta\Omega_b^* & \delta & R_1\eta\Omega_r & & & 0 \\ 0 & R_1\eta\Omega_r^* & 0 & & & 0 \\ \vdots & & & \ddots & & \vdots \\ 0 & & & & \delta & R_{N-1}\eta\Omega_r \\ 0 & & \cdots & & R_{N-1}\eta\Omega_r^* & 0 \end{pmatrix}$$

with a basis of $\{|D_N^0\rangle_s|0\rangle_p, |D_N^1\rangle_s|1\rangle_p, \ldots, |D_N^{N-1}\rangle_s|1\rangle_p, |D_N^N\rangle_s|0\rangle_p\}$.

In this Letter, we consider only even numbers of ions. This allows us to calculate the dark state $|\psi_d(\Omega_r, \Omega_b)\rangle$ [15,16] as

$$|\psi_d(\Omega_r, \Omega_b)\rangle = A \sum_{i=0}^{N/2} C_i \Omega_b^i \Omega_r^{N/2-i} |D_N^{2i}\rangle_s |0\rangle_m,$$

$$C_0 = 1, \qquad C_i = (-1)^i \prod_{j=1}^i \frac{R_{2j-2}}{R_{2j-1}}, \qquad @\left(i=1,\ldots\frac{N}{2}\right),$$

where A is a normalizing constant. The dark state exists only for the motional ground state.

Since each dark state (except for the initial and final states) is a superposition of states which are connected due to the quadratic raising and lowering operators of $\hat{J}_+\hat{J}_+$ and $\hat{J}_-\hat{J}_-$, the dark states correspond to the vacuum squeezed state in quantum optics [13,17]. To see these characteristics, we calculate the spin noise for the four-ion case. Figure 1(b) shows the dependence of the variance of the global spin operator $[\Delta\hat{J}_k^2$ $(k = x, y, z)]$ for dark states on the parameter θ ($\Omega_b = 1 - \cos\theta$, $\Omega_r = 1 + \cos\theta$). For $0 < \theta < \frac{\pi}{2}$ or $\frac{\pi}{2} < \theta < \pi$, the spin noises are squeezed or antisqueezed and when $\theta = \frac{\pi}{2}$ ($\Omega_b = \Omega_r$), the spin noise in one direction goes to zero and the half-excited symmetric Dicke state in the x direction ($|D_{4,x}^2\rangle = \hat{R}_y(\pi/2)|D_4^2\rangle$) is generated, where $\hat{R}_y(\theta)$ is the global rotation operator about the y axis. Even for the general case of $2n$ ions, the half-excited symmetric Dicke state ($|D_{2n,x}^n\rangle$) is generated when $\Omega_b = \Omega_r$ because the dark state $|\psi_d(\Omega, \Omega)\rangle$ is the eigenstate of the angular momentum operator in the x direction $[\hat{J}_x = (\hat{J}_+ + \hat{J}_-)/2]$

$$\hat{J}_x|\psi_d(\Omega, \Omega)\rangle = 0.$$

This population transfer using the dark states of phonon-mediated multilevel Raman transitions is robust against phase fluctuations of qubits due to stray magnetic fields or a laser linewidth because the quantum state is always in the dark state of the Hamiltonian, as in the STIRAP method [18,19].

We demonstrate phonon-mediated STIRAP with two and four calcium ions trapped in a linear Paul trap. Details of the experimental system used are described in our previous studies [14,20]. The center-of-mass mode of the axial direction is cooled by sideband cooling to the ground state ($n_{\mathrm{COM}} \sim 0.02$), while the other motional modes are cooled only by Doppler cooling. The qubit is composed of a ground state $S_{1/2}$ ($m = -1/2$) and a metastable state $D_{5/2}$ ($m' = -5/2$) of a calcium ion, and we use $S_{1/2} - D_{5/2}$ transitions to excite sideband transitions. To measure the spin projection and population of each spin state, we use a photomultiplier and the electron-shelving method with fluorescence discrimination using a threshold, which is 80 counts per ion. We first initialize all the qubits by optical pumping and irradiate them only with the red sideband laser pulse so that the initial state becomes the dark state. To operate phonon-mediated STIRAP, we change the amplitude of the sideband pulses, as shown in Fig. 2(a). The peak Rabi frequency of the transitions is $\eta\Omega = 2\pi \times 14$ kHz and the pulse length is $\tau = 340$ μs. The adiabatic condition is satisfied as $\eta\Omega\tau \sim 5 > 1$ [15]. Figure 2(b) shows the measured spin projection $\langle\hat{J}_z\rangle$ during population transfer for the four-ion case where a high-efficiency transfer is demonstrated. To see the characteristics of spin squeezing, the time evolution of the variance
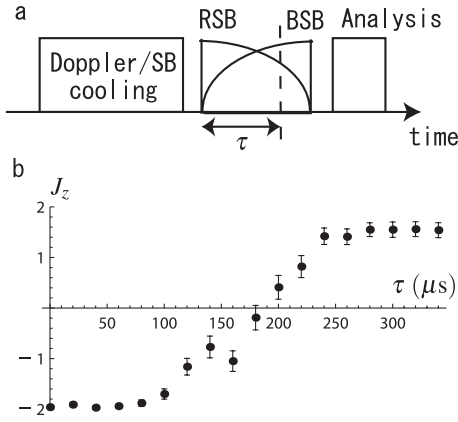
FIG. 2.   (a) Pulse sequences for phonon-mediated STIRAP. We measure the evolution of spin and spin noise by truncating the STIRAP pulse after time τ. (b) Time evolution of population transfer from the $|\downarrow\downarrow\downarrow\downarrow\rangle$ state to the $|\uparrow\uparrow\uparrow\uparrow\rangle$ state.

of the global spin operator is measured. It is shown in Fig. 3 for four ions. This shows that the spin noises are squeezed or antisqueezed.

When the two sideband pulses have the same amplitude, the half-excited symmetric Dicke state given by

$$|D_{2,x}^1\rangle = \frac{1}{\sqrt{2}}(|D_2^0\rangle - |D_2^2\rangle),$$

$$|D_{4,x}^2\rangle = \sqrt{\frac{3}{8}}|D_4^0\rangle - \sqrt{\frac{1}{4}}|D_4^2\rangle + \sqrt{\frac{3}{8}}|D_4^4\rangle$$

is generated. We evaluate these half-excited symmetric Dicke states for the two- and four-ion cases.
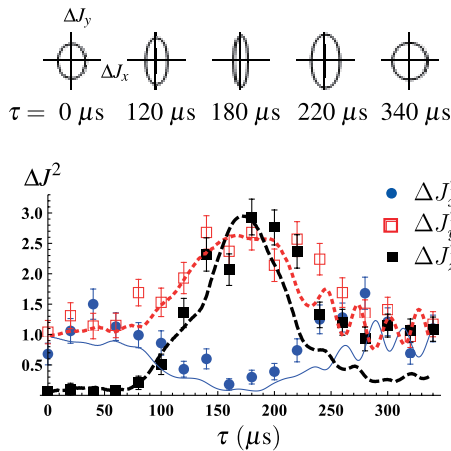

FIG. 3 (color online).   (upper) Visualized experimental spin noise in XY plane, which evolves with phonon-mediated STIRAP. (lower) Time evolution of spin noise. Blue circles, red open squares, and black closed squares indicate ΔJ_x^2, ΔJ_y^2, and ΔJ_z^2, respectively. J_x (J_y and J_z) is (anti)squeezed. Curves are numerical calculations for J_x (blue solid), J_y (red dotted), and J_z (black dashed).

For the two-ion case, because the Dicke state is the same as one of the Bell states, we can estimate the fidelity only with a global operation and by measuring a parity oscillation. When $\Omega_r = \Omega_b$, we irradiate the ions with a $\pi/2$ pulse whose phase is ϕ and measure the expectation value of a parity operator. Figure 4(a) shows the parity oscillation; its amplitude is estimated to be $A_p = 0.95 \pm 0.05$ by fitting. Without the $\pi/2$ pulse, the diagonal elements are measured to be $\{p_{-1}, p_0, p_1\} = \{0.516, 0.033, 0.451\} \pm \{0.011, 0.004, 0.011\}$. Using these values, we can obtain the fidelity as $F = \frac{p_{-1}+p_1+A_p}{2} = 0.96 \pm 0.03$, which is higher than 0.5 [21].

To evaluate the four-ion Dicke state, we use (i) witness and (ii) fidelity methods. For genuine four-partite entangled states, the witness operator with global spin operators is given by [22]

$$\hat{W}_{ij} = \left(\frac{7}{2} + \sqrt{3}\right)\hat{1} - (\hat{J}_i^2 + \hat{J}_j^2) \sim 5.23 \cdot \hat{1} - (\hat{J}_i^2 + \hat{J}_j^2),$$

where i and j are any two orthogonal directions. For the Dicke state in the x direction ($|D_{2n,x}^n\rangle$), we can evaluate its entanglement with the witness $\hat{W}_{yz}$. After phonon-mediated STIRAP for four ions, we irradiate the ions with a $\pi/2$ pulse whose phase is ϕ and measure the expectation values of the square of the spin J_ϕ^2 [see Fig. 4(b)]. This maximum peak (2.64 ± 0.05) corresponds to $\langle \hat{J}_y^2 \rangle$. On the other hand, $\langle \hat{J}_z^2 \rangle$ is measured as 2.82 ± 0.05 without an analysis pulse. The witness is then calculated as

$$\langle \hat{W}_{yz} \rangle = -0.23 \pm 0.07 < 0,$$

which is smaller than 0 by more than σ. This supports generation of genuine four-partite entanglement [22].

We also evaluate the Dicke state with a bound on the fidelity, which is important to demonstrate that the generated
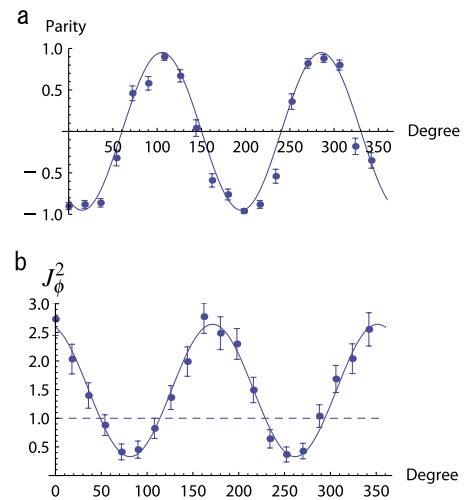

FIG. 4 (color online).   (a) Parity oscillation of the Dicke state of two ions. (b) Squared spin of the half-excited Dicke state of four ions. The dashed line indicates shot noise for four ions.

state is closer to the Dicke state than the other genuine four-partite entangled states. For the Dicke state, the fidelity cannot be exactly determined without full quantum tomography [23], which requires local access and many measurements [24]. Here, we evaluate the lower and upper bounds of the fidelity, rather than the fidelity, by using only global access and a few measurements. Details of this method are described in the Appendix. For the four-ion case, the fidelity (F) of the half-excited symmetric Dicke state along the x direction is bounded such that

$$\frac{\langle \hat{J}_y^2 \rangle + \langle \hat{J}_z^2 \rangle}{4} - \left[\frac{p_{-2}^{(x)} + p_2^{(x)} + p_0^{(x)}}{2} + \frac{5(p_{-1}^{(x)} + p_1^{(x)})}{4} \right] \leq F \leq p_0^{(x)},$$

where $p_i^{(x)}$ is the population of the angular momentum state whose spin component along the x direction is i. When $\Omega_r = \Omega_b$, we measure $p_i^{(x)}$ as $\{p_{-2}^{(x)}, p_{-1}^{(x)}, p_0^{(x)}, p_1^{(x)}, p_2^{(x)}\} = \{0.00, 0.03, 0.88, 0.03, 0.03\} \pm \{0.00, 0.02, 0.03, 0.02, 0.02\}$. From these populations and witness, we evaluate the fidelity as

$$0.84 \pm 0.03 \leq F \leq 0.88 \pm 0.03.$$

The infidelities mainly come from the initial mean phonon number of the COM mode and the ac Stark shifts from the two-color laser beams. In the experiments the initial mean phonon number of the COM mode is 0.02 and that means the maximum fidelity of Dicke states is 0.98. Second sweeping the amplitudes of the two-color laser beams induces time-dependent ac Stark shifts, which are a few kilohertz at maximum. The variation of the ac Stark shifts breaks the adiabatic condition and reduces the fidelity. We numerically calculate the effect of such time-dependent ac Stark shifts using experimental parameters and the fidelity goes down to 0.90 for the four-ion case without other infidelity. To avoid this effect, we can increase the secular frequency of the ion's motion, or simultaneously irradiate ions with an additional laser beam to compensate the ac Stark shifts.

In summary, we demonstrate phonon-mediated STIRAP and generate the half-excited Dicke states of two and four ions. This method requires only the motional ground state and global access to whole ions. Moreover, the adiabatic process, which corresponds to the spin squeezing operation, makes the method robust against certain disturbances and high-fidelity Dicke states can be generated. The fidelity of these Dicke states are measured as $F = 0.96 \pm 0.03$ for two ions and $0.84 \pm 0.03 \leq F \leq 0.88 \pm 0.03$ for four ions. Using the witness operator, we show that the generated four-ion state is a genuine four-qubit entangled state and, from the lower bound of the fidelity, we show that this state is the half-excited symmetric Dicke state.

APPENDIX

We calculate the upper and lower bounds of the fidelity of the half-excited Dicke states ($|D_{2n}^n\rangle$). We suppose that the square of global spin operators ($\langle \hat{J}_x^2 \rangle + \langle \hat{J}_y^2 \rangle$) and the population of the angular momentum state along the z axis have been measured:

$$W_0 = \langle \hat{J}_x^2 \rangle + \langle \hat{J}_y^2 \rangle = \langle \hat{J}^2 \rangle - \langle \hat{J}_z^2 \rangle,$$
$$P = \{p_{-j_m}, p_{-j_m+1}, \ldots, p_0, \ldots, p_{j_m}\},$$

where j_m is the maximum projection along the z axis, which is equal to the ion number divided by 2. We consider the diagonal elements of the density matrix based on the angular momentum state along the z axis:

$$\rho_{j, j_z, \xi} = \langle \xi; j, j_z | \hat{\rho} | \xi; j, j_z \rangle,$$

where $|\xi; j, j_z\rangle$ satisfies $\hat{J}^2 |\xi; j, j_z\rangle = j(j + 1)|\xi; j, j_z\rangle$ and $\hat{J}_z |\xi; j, j_z\rangle = j_z |\xi; j, j_z\rangle$. $\xi (= 1, 2, \ldots)$ is an index expressing the array of the intermediate angular momentums when we couple the angular momentum. States with $j = j_m$ comprise only these perfectly symmetric states. We then assume that the states $|\xi = 1; j = j_m, j_z\rangle$ are symmetric Dicke states. We can calculate the population P such that $p_{j_z} = \sum_{j,\xi} \rho_{j, j_z, \xi}$. Note that $\rho_{j_m, 0, 1}$ is the fidelity of the half-excited Dicke state.

For the upper bound, we expand p_0 as

$$p_0 = \sum_{j,\xi} \rho_{j, 0, \xi} \geq \rho_{j_m, 0, 1} = F$$

because the diagonal elements of the density matrix are non-negative ($\rho_{j, j_z, \xi} \geq 0$).

As W_0 is diagonalized by the angular momentum state along the z axis, we have

$$W_0 = \sum_{j, j_z, \xi} [j(j + 1) - j_z^2] \rho_{j, j_z, \xi}$$
$$\leq \sum_{j, \xi} j(j + 1) \rho_{j, 0, \xi} + \sum_{j_z \neq 0} [j_m(j_m + 1) - j_z^2] p_{j_z}.$$

The first term on the right-hand side is again bounded as

$$\sum_{j, \xi} [j(j + 1)] \rho_{j, 0, \xi}$$
$$\leq j_m(j_m + 1) \rho_{j_m, 0, 1} + (j_m - 1) j_m \sum_{j \neq j_m, \xi} \rho_{j, 0, \xi}$$
$$\leq j_m(j_m + 1) \rho_{j_m, 0, 1} + (j_m - 1) j_m (p_0 - \rho_{j_m, 0, 1}).$$

Using these inequalities, the fidelity has the following lower bound:

$$\frac{W_0}{2j_m} - \frac{j_m - 1}{2} p_0 - \sum_{j_z \neq 0} \left(\frac{j_m + 1}{2} - \frac{j_z^2}{2j_m} \right) p_{j_z} \leq F.$$

*noguchi@qe.ee.es.osaka-u.ac.jp

[1] T. Monz, P. Schindler, J. Barreiro, M. Chwalla, D. Nigg, W. Coish, M. Harlander, W. Hänsel, M. Hennrich, and R. Blatt, Phys. Rev. Lett. **106**, 130506 (2011).

[2] K. Molmer and A. Sorensen, Phys. Rev. Lett. **82**, 1835 (1999).

[3] N. Kiesel, C. Schmid, G. Toth, E. Solano, and H. Weinfurter, Phys. Rev. Lett. **98**, 063604 (2007).

[4] W. Wieczorek, R. Krischek, N. Kiesel, P. Michelberger, G. Tóth, and H. Weinfurter, Phys. Rev. Lett. **103**, 020504 (2009).

[5] I. E. Linington and N. V. Vitanov, Phys. Rev. A **77**, 010302 (2008).

[6] I. E. Linington and N. V. Vitanov, Phys. Rev. A **77**, 062327 (2008).

[7] H. Häffner et al., Nature (London) **438**, 643 (2005).

[8] D. N. Matsukevich, T. Chanelière, M. Bhattacharya, S.-Y. Lan, S. Jenkins, T. Kennedy, and A. Kuzmich, Phys. Rev. Lett. **95**, 040405 (2005).

[9] D. J. Wineland, J. J. Bollinger, W. M. Itano, and D. J. Heinzen, Phys. Rev. A **50**, 67 (1994).

[10] T. Kim, O. Pfister, M. J. Holland, J. Noh, and J. L. Hall, Phys. Rev. A **57**, 4004 (1998).

[11] B. Lücke et al., Science **334**, 773 (2011).

[12] C. D. Hamley, C. S. Gerving, T. M. Hoang, E. M. Bookjans, and M. S. Chapman, Nat. Phys. **8**, 305 (2012).

[13] G. S. Agarwal and R. R. Puri, Phys. Rev. A **41**, 3782 (1990).

[14] A. Noguchi, S. Haze, K. Toyoda, and S. Urabe, Phys. Rev. Lett. **108**, 060503 (2012).

[15] B. W. Shore, K. Bergmann, J. Oreg, and S. Rosenwaks, Phys. Rev. A **44**, 7442 (1991).

[16] N. V. Vitanov, T. Halfmann, B. W. Shore, and K. Bergmann, Annu. Rev. Phys. Chem. **52**, 763 (2001).

[17] T. Hirano and M. Matsuoka, Opt. Lett. **15**, 1153 (1990).

[18] R. Unanyan, M. Fleischhauer, B. W. Shore, and K. Bergmann, Opt. Commun. **155**, 144 (1998).

[19] N. Timoney, I. Baumgart, M. Johanning, A. F. Varón, M. B. Plenio, A. Retzker, and C. Wunderlich, Nature (London) **476**, 185 (2011).

[20] K. Toyoda, T. Watanabe, T. Kimura, S. Nomura, S. Haze, and S. Urabe, Phys. Rev. A **83**, 022315 (2011).

[21] C. A. Sackett et al., Nature (London) **404**, 256 (2000).

[22] G. Toth, J. Opt. Soc. Am. B **24**, 275 (2007).

[23] L.-M. Duan, Phys. Rev. Lett. **107**, 180502 (2011).

[24] M. Cramer, M. B. Plenio, S. T. Flammia, R. Somma, D. Gross, S. D. Bartlett, O. Landon-Cardinal, D. Poulin, and Y.-K. Liu, Nat. Commun. **1**, 149 (2010).